

Article

Rényi and Tsallis entropies of the Aharonov-Bohm ring in uniform magnetic fields

O. Olendski ^{1,†}  0000-0001-7891-1793

¹ Department of Applied Physics and Astronomy, University of Sharjah, P.O. Box 27272, Sharjah, United Arab Emirates; e-mail: oolendski@sharjah.ac.ae

Version October 25, 2019 submitted to Entropy

Abstract: One-parameter functionals of the Rényi $R_{\rho,\gamma}(\alpha)$ and Tsallis $T_{\rho,\gamma}(\alpha)$ types are calculated both in the position (subscript ρ) and momentum (γ) spaces for the azimuthally symmetric 2D nanoring that is placed into the combination of the transverse uniform magnetic field \mathbf{B} and the Aharonov-Bohm (AB) flux ϕ_{AB} and whose potential profile is modelled by the superposition of the quadratic and inverse quadratic dependencies on the radius r . Position (momentum) Rényi entropy depends on the field B as a negative (positive) logarithm of $\omega_{eff} \equiv (\omega_0^2 + \omega_c^2/4)^{1/2}$, where ω_0 determines the quadratic steepness of the confining potential and ω_c is a cyclotron frequency. This makes the sum $R_{\rho_{nm}}(\alpha) + R_{\gamma_{nm}}(\frac{\alpha}{2\alpha-1})$ a field-independent quantity that increases with the principal n and azimuthal m quantum numbers and does satisfy corresponding uncertainty relation. In the limit $\alpha \rightarrow 1$ both entropies in either space tend to their Shannon counterparts along, however, different paths. Analytic expression for the lower boundary of the semi-infinite range of the dimensionless coefficient α where the momentum entropies exist reveals that it depends on the ring geometry, AB intensity and quantum number m . It is proved that there is the only orbital for which both Rényi and Tsallis uncertainty relations turn into the identity at $\alpha = 1/2$ and which is not necessarily the lowest-energy level. At any coefficient α , the dependence of the position Rényi entropy on the AB flux mimics the energy variation with ϕ_{AB} what, under appropriate scaling, can be used for the unique determination of the associated persistent current. Similarities and differences between the two entropies and their uncertainty relations are discussed too.

Keywords: quantum ring; Rényi entropy; Tsallis entropy; magnetic field; Aharonov-Bohm effect

1. Introduction

In an attempt to expand quantum-information theory to the study of the QRs [1], recent analysis [2] addressed an influence of the combination of the transverse uniform magnetic field \mathbf{B} and the AB flux ϕ_{AB} [3] on the position and momentum components of, among others, Shannon entropy [4] of the one-particle orbitals of the flat 2D annulus whose rotationally symmetric potential profile $U(r)$ is modelled in the position polar coordinates (r, φ_r) by the superposition of the quadratic and inverse quadratic dependencies on the radius r [5–15]:

$$U(r) = \frac{1}{2}m^*\omega_0^2r^2 + \frac{\hbar^2}{2m^*r^2}a - \hbar\omega_0a^{1/2}, \quad (1)$$

where m^* is an effective mass of a charge carrier, frequency ω_0 defines a steepness of the confining in-plane outer surface of the QR with its characteristic radius $r_0 = [\hbar/(2m^*\omega_0)]^{1/2}$, and positive dimensionless constant a describes a strength of the repulsive potential near the origin. General definition

of the Shannon position S_ρ and momentum S_γ quantum-information entropies in the l -dimensional spaces read:

$$S_\rho = - \int_{\mathbb{R}^l} \rho(\mathbf{r}) \ln \rho(\mathbf{r}) d\mathbf{r} \quad (2a)$$

$$S_\gamma = - \int_{\mathbb{R}^l} \gamma(\mathbf{k}) \ln \gamma(\mathbf{k}) d\mathbf{k}, \quad (2b)$$

with the integration carried out over the whole available regions where the corresponding waveforms $\Psi(\mathbf{r})$ and $\Phi(\mathbf{k})$ that enter into the densities

$$\rho(\mathbf{r}) = |\Psi(\mathbf{r})|^2 \quad (3a)$$

$$\gamma(\mathbf{k}) = |\Phi(\mathbf{k})|^2, \quad (3b)$$

are defined. Position $\Psi(\mathbf{r})$ and wave vector $\Phi(\mathbf{k})$ functions are related to each other through the Fourier transformation what for the 2D geometry of the QR is expressed as:

$$\Phi_{nm}(k, \varphi_k) = \frac{1}{2\pi} \int_0^{2\pi} d\varphi_r \int_0^\infty dr r \Psi_{nm}(r, \varphi_r) e^{-ikr \cos(\varphi_r - \varphi_k)} \quad (4a)$$

$$\Psi_{nm}(r, \varphi_r) = \frac{1}{2\pi} \int_0^{2\pi} d\varphi_k \int_0^\infty dk k \Phi_{nm}(k, \varphi_k) e^{ikr \cos(\varphi_k - \varphi_r)}, \quad (4b)$$

where (k, φ_k) are the wave vector polar coordinates and $n = 0, 1, 2, \dots$, and $m = 0, \pm 1, \pm 2, \dots$, are principal and azimuthal indices, respectively. Due to the rotational symmetry of the QR, either dependence is most conveniently represented as a product of the angular and radial parts:

$$\Psi_{nm}(r, \varphi_r) = \frac{1}{(2\pi)^{1/2}} e^{im\varphi_r} R_{nm}(r) \quad (5a)$$

$$\Phi_{nm}(k, \varphi_k) = \frac{(-i)^m}{(2\pi)^{1/2}} e^{im\varphi_k} K_{nm}(k), \quad (5b)$$

where the latter ones are:

$$R_{nm}(r) = \frac{1}{r_{eff}} \left[\frac{n!}{\Gamma(n+\lambda+1)} \right]^{1/2} \exp\left(-\frac{1}{4} \frac{r^2}{r_{eff}^2}\right) \left(\frac{1}{2} \frac{r^2}{r_{eff}^2}\right)^{\lambda/2} L_n^\lambda\left(\frac{1}{2} \frac{r^2}{r_{eff}^2}\right) \quad (6a)$$

$$K_{nm}(k) = r_{eff} \left[\frac{n!}{\Gamma(n+\lambda+1)} \right]^{1/2} \int_0^\infty e^{-z/2} z^{\lambda/2} L_n^\lambda(z) J_{|m|}\left(2^{1/2} r_{eff} k z^{1/2}\right) dz. \quad (6b)$$

Here, $\Gamma(x)$, $L_n^\alpha(x)$ and $J_m(x)$ are Γ -function, generalized Laguerre polynomial and m -th order Bessel function of the first kind, respectively [16,17]. In addition,

$$r_{eff} = \left(\frac{\hbar}{2m^* \omega_{eff}} \right)^{1/2} \quad (7a)$$

$$\omega_{eff} = \left(\omega_0^2 + \frac{1}{4} \omega_c^2 \right)^{1/2} \quad (7b)$$

and

$$\omega_c = \frac{eB}{m^*} \quad (7c)$$

is the cyclotron frequency,

$$\lambda = \left(m_\phi^2 + a\right)^{1/2} \quad (7d)$$

$$m_\phi = m + \nu \quad (7e)$$

with ν being a dimensionless AB flux, i.e., the latter one is expressed in units of the elementary flux quantum $\phi_0 = h/e$:

$$\nu = \frac{\phi_{AB}}{\phi_0}. \quad (7f)$$

It is easy to check that both function sets are orthonormalized:

$$\begin{aligned} & \int_0^{2\pi} d\varphi_r \int_0^\infty dr r \Psi_{n'm'}^*(r, \varphi_r) \Psi_{nm}(r, \varphi_r) \\ &= \int_0^{2\pi} d\varphi_k \int_0^\infty dk k \Phi_{n'm'}^*(k, \varphi_k) \Phi_{nm}(k, \varphi_k) = \delta_{nn'} \delta_{mm'}, \end{aligned} \quad (8)$$

20 where $\delta_{nn'}$ is a Kronecker delta.

It was shown [2] that Shannon position (momentum) quantum information entropy decreases (increases) with the growing field B as $\pm 2 \ln r_{eff}$ what physically means that in the corresponding space there is more (less) information about the particle location (intensity of motion). As a result, the sum $S_\rho + S_\gamma$, describing a total amount of the simultaneous information about the charge carrier, can not be altered by the uniform magnetic component and it does always satisfy the fundamental restriction [18,19]:

$$S_\rho + S_\gamma \geq l(1 + \ln \pi); \quad (9)$$

in particular, for our geometry this uncertainty relation becomes tight for the lowest level, $n = m = 0$, of the AB-free, $\phi_{AB} = 0$, QD, $a = 0$: mathematically, Eqs. (6) at the zero values of n , ϕ_{AB} and a degenerate to

$$R_{0m}(r)|_{a=\nu=0} = \frac{1}{r_{eff}} \frac{1}{(|m|!)^{1/2}} \left(\frac{r}{2^{1/2} r_{eff}}\right)^{|m|} \exp\left(-\frac{1}{4} \frac{r^2}{r_{eff}^2}\right) \quad (10a)$$

$$K_{0m}(k)|_{a=\nu=0} = 2r_{eff} \frac{1}{(|m|!)^{1/2}} \left(2^{1/2} r_{eff} k\right)^{|m|} \exp\left(-r_{eff}^2 k^2\right), \quad (10b)$$

what means that at $a = \nu = 0$ the functions $\Psi_{00}(\mathbf{r})$ and $\Phi_{00}(\mathbf{k})$ turn into the 2D Gaussians converting relation (9) into the equality. Next, a dependence of the position entropy S_ρ on the normalized AB flux ν strongly resembles that of the energy spectrum:

$$E_{nm}(a, \nu; \omega_c) = \hbar\omega_{eff} (2n + \lambda + 1) + \frac{1}{2} m_\phi \hbar\omega_c - \hbar\omega_0 a^{1/2}. \quad (11)$$

Accordingly, the knowledge of $S_\rho - \nu$ characteristics permits to calculate the persistent current [20], which is a negative derivative of the energy with respect to the AB intensity:

$$J_{nm} \equiv -\frac{e}{\hbar} \frac{\partial E}{\partial m} \equiv -\frac{\partial E}{\partial \phi_{AB}} = -\frac{e\omega_0}{2\pi} \left[\frac{m\phi}{\lambda} \sqrt{1 + \frac{1}{4} \left(\frac{\omega_c}{\omega_0} \right)^2} + \frac{1}{2} \frac{\omega_c}{\omega_0} \right]. \quad (12)$$

For many years, physicists and mathematicians have been looking for and discussing generalizations of the Shannon measures from Eqs. (2). Notably, two most famous and frequently used outcomes of these endeavors are one-parameter functionals of the Rényi $R_{\rho,\gamma}(\alpha)$ ¹ [21,22]

$$R_\rho(\alpha) = \frac{1}{1-\alpha} \ln \left(\int_{\mathbb{R}^l} \rho^\alpha(\mathbf{r}) d\mathbf{r} \right) \quad (13a)$$

$$R_\gamma(\alpha) = \frac{1}{1-\alpha} \ln \left(\int_{\mathbb{R}^l} \gamma^\alpha(\mathbf{k}) d\mathbf{k} \right) \quad (13b)$$

and Tsallis $T_{\rho,\gamma}(\alpha)$ [23] (or, more correctly, Havrda-Charvát-Daróczy-Tsallis [24,25])

$$T_\rho(\alpha) = \frac{1}{\alpha-1} \left(1 - \int_{\mathbb{R}^l} \rho^\alpha(\mathbf{r}) d\mathbf{r} \right) \quad (14a)$$

$$T_\gamma(\alpha) = \frac{1}{\alpha-1} \left(1 - \int_{\mathbb{R}^l} \gamma^\alpha(\mathbf{k}) d\mathbf{k} \right) \quad (14b)$$

types, where a non-negative coefficient $0 \leq \alpha < \infty$ controls the reaction of the system to its deviation from the equilibrium; namely, the l'Hôpital's rule deduces that at $\alpha \rightarrow 1$ both Rényi and Tsallis entropies degenerate to their Shannon counterpart, Eqs. (2), whereas at the vanishingly small magnitudes, this parameter allows equal contributions from the random events of any frequency of actual occurrence what in the case of the infinite or semi-infinite region of integration in Eqs. (13) and (14) leads to the divergence of the corresponding measure (provided it exists) at $\alpha \rightarrow 0$. On the other hand, extremely strong Rényi or Tsallis parameters pick up in the corresponding probability distributions the global maxima only with a full discard of all other happenings. Using similar arguments, it can be shown that both entropies are decreasing functions of their factor α . Let us mention another particular case of these entropies; namely, Onicescu energies [26], or disequilibria,

$$O_\rho = \int_{\mathbb{R}^l} \rho^2(\mathbf{r}) d\mathbf{r} \quad (15a)$$

$$O_\gamma = \int_{\mathbb{R}^l} \gamma^2(\mathbf{k}) d\mathbf{k}, \quad (15b)$$

which describe deviations from the uniform distributions, are expressed with the help of Eqs. (13) and (14) as

$$O_{\rho,\gamma} \equiv e^{-R_{\rho,\gamma}(2)} \equiv 1 - T_{\rho,\gamma}(2). \quad (16)$$

- 21 For the QR, the position (momentum) Onicescu energy increases (decreases) with the uniform field as
 22 r_{eff}^{-2} (r_{eff}^2) what makes the product $O_\rho O_\gamma$, similar to the sum $S_\rho + S_\gamma$, a B -independent quantity [2].

¹ To tell the Rényi entropies from the radial part of the position waveform, Eq. (6a), we will always write the former ones with the subscript ρ or γ denoting a corresponding space.

Sobolev inequality of the conjugated Fourier transforms [27]

$$\left(\frac{\alpha}{\pi}\right)^{l/(4\alpha)} \left[\int_{\mathbb{R}^l} \rho^\alpha(\mathbf{r}) d\mathbf{r} \right]^{1/(2\alpha)} \geq \left(\frac{\beta}{\pi}\right)^{l/(4\beta)} \left[\int_{\mathbb{R}^l} \gamma^\beta(\mathbf{k}) d\mathbf{k} \right]^{1/(2\beta)} \quad (17)$$

with the non-negative coefficients α and β obeying the constraint:

$$\frac{1}{\alpha} + \frac{1}{\beta} = 2, \quad (18)$$

supplemented by the additional requirement

$$\frac{1}{2} \leq \alpha \leq 1, \quad (19)$$

directly establishes the uncertainty relation between the position and momentum Tsallis entropies for each bound quantum orbital [28]:

$$\left(\frac{\alpha}{\pi}\right)^{l/(4\alpha)} [1 + (1 - \alpha)T_\rho(\alpha)]^{1/(2\alpha)} \geq \left(\frac{\beta}{\pi}\right)^{l/(4\beta)} [1 + (1 - \beta)T_\gamma(\beta)]^{1/(2\beta)}. \quad (20)$$

Logarithmization of Eq. (17) yields the following inequality for the Rényi components [29,30]:

$$R_\rho(\alpha) + R_\gamma(\beta) \geq -\frac{l}{2} \left(\frac{1}{1 - \alpha} \ln \frac{\alpha}{\pi} + \frac{1}{1 - \beta} \ln \frac{\beta}{\pi} \right), \quad (21)$$

for which the restriction from Eq. (19) is waived. Note that near its unity, the Tsallis parameter turns the corresponding uncertainty, Eq. (20), into

$$\frac{1 + [-2S_\rho + l(1 + \ln \pi)] (\alpha - 1)/4}{\pi^{l/4}} \geq \frac{1 + [2S_\gamma - l(1 + \ln \pi)] (\alpha - 1)/4}{\pi^{l/4}}, \quad \alpha \rightarrow 1, \quad (22)$$

23 what means that, first, at $\alpha = 1$ it becomes an identity with each of its sides equal to dimensionless $\pi^{-l/4}$
 24 [what follows though directly from Eq. (17)] and, second, due to the Beckner-Białynicki-Birula-Mycielski
 25 inequality [18,19], Eq. (9), the relation from Eq. (22) turns into the strict inequality at $\alpha < 1$ only, as
 26 stated above, Eq. (19). At the same time, its Rényi counterpart, Eq. (21), with the help of the l'Hôpital's
 27 rule degenerates in the limit $\alpha \rightarrow 1$ (and, accordingly, $\beta \rightarrow 1$) into its Shannon fellow, Eq. (9). It was
 28 conjectured [31] that the inequalities from Eqs. (17), (20) and (21) for the lowest-energy level turn into the
 29 identities at $\alpha = 1/2$. This issue will be addressed below. Important difference between the entropies is
 30 the fact that the Rényi and Shannon functionals are additive (or extensive) whereas the Tsallis dependence
 31 is not. More information on each of the entropies can be found in many sources; see, e.g., Refs. [32–35].

32 Unique properties of the Rényi and Tsallis entropies explain their wide applications in almost every
 33 branch of science and other fields of human activity: from seismology [36] and ecology [37,38] with
 34 geography [39] through medicine [40,41] and biology [42] to quantum physics [43–52], free field theories
 35 [53,54] and astronomy [55] with many, many others in between and beyond. Partially relevant to our
 36 discussion, let us point out that, in the latest development, very recent experiments on Bose-Einstein
 37 condensate of interacting ^{87}Rb atoms loaded into a 1D [56] or 2D [57] optical lattice and on up to twenty
 38 $^{40}\text{Ca}^+$ ions trapped into 1D straight string [58] directly measured the Rényi entanglement entropy with
 39 $\alpha = 2$ of these many-body systems. These state-of-the-art achievements open up new perspectives in

40 probing and describing dynamics of correlated qubits and simultaneously raise new challenges for the
41 correct theoretical description of the Rényi and Tsallis entropies of the miscellaneous quantum structures.

42 In the present research, a comprehensive description of both measures is provided for the QR with
43 the potential profile described by Eq. (1) placed into the superposition of the uniform \mathbf{B} and AB ϕ_{AB}
44 magnetic fields with special emphasis being paid to the derivation of the analytic results; for example,
45 even though the expressions for the momentum components of the entropies in general can be evaluated
46 numerically only, it is possible to get a simple formula for the lower boundary α_{TH} of the semi-infinite
47 range of the Rényi or Tsallis coefficient at which the integrals in Eqs. (13b) and (14b) converge. Its
48 inspection reveals that the QD momentum functionals exist at any non-negative α whereas for the QR
49 topology the threshold is determined not only by the potential (or, more precisely, by the antidot strength
50 a) but also by the orbital itself. In addition, the AB flux is the only external agent that can control this
51 boundary since α_{TH} does not depend on B . The paths along which both entropies approach at $\alpha \rightarrow 1$
52 their Shannon counterpart are shown to be different for the Rényi and Tsallis measures. Limiting cases
53 of the extremely small and infinitely large coefficient α are also addressed. Next, neither Rényi nor
54 Tsallis uncertainty relation depends on the uniform field \mathbf{B} . Since the lowest-orbital position $\Psi_{00}(\mathbf{r})$ and
55 wave vector $\Phi_{00}(\mathbf{k})$ functions of the AB-free QD ($\nu = a = 0$) are described by the 2D Gaussians, the
56 corresponding inequalities, Eq. (20) and (21), are saturated for this level at any coefficient α ; in particular,
57 for the Tsallis case a restraint from Eq. (19) is waived. The $n = m = 0$ state is a special one also for the QR
58 since it is the only orbital that at $\alpha = 1/2$ turns Eq. (20) and (21) into the identities. The dependence of
59 the measures on the AB intensity is investigated too and it is shown that since the position Rényi entropy
60 at any coefficient α qualitatively repeats the energy dependence on the flux, its knowledge can be useful
61 in predicting the associated persistent currents.

62 Structure of the research presented below is as follows. Measures properties in the uniform magnetic
63 field are discussed in Sec. 2 where their position and momentum components are addressed first in
64 subsections 2.1 and 2.2, respectively, whereas the uncertainty relations are studied in subsection 2.3,
65 which is divided into parts devoted to the Tsallis and Rényi functionals. Sec. 3 contains an analysis
66 of the Rényi entropies dependence on the AB flux and its relevance to the prediction of the magnitude of
67 the persistent currents. Discussion is wrapped up in Sec. 4 by some concluding remarks.

68 2. Entropies in uniform magnetic field \mathbf{B}

69 2.1. Position components

Inserting the forms of the wave functions from Eqs. (5) and (6) into the general definition of the Rényi, Eqs. (13), and Tsallis, Eqs. (14), entropies yields:

$$R_{\rho_{nm}}(\alpha) = 2 \ln r_{eff} + \ln 2\pi + \frac{1}{1-\alpha} \ln \left(\left[\frac{n!}{\Gamma(n+\lambda+1)} \right]^\alpha \frac{1}{\alpha^{\lambda+1}} \int_0^\infty e^{-z} z^{\alpha\lambda} \left[L_n^\lambda \left(\frac{z}{\alpha} \right)^2 \right]^\alpha dz \right) \quad (23a)$$

$$R_{\gamma_{nm}}(\alpha) = -2 \ln r_{eff} + \ln 2\pi + \frac{\alpha}{\alpha-1} \ln \frac{n!}{\Gamma(n+\lambda+1)} + \frac{1}{1-\alpha} \ln \int_0^\infty d\xi \zeta \left(\left[\int_0^\infty e^{-z/2} z^{\lambda/2} L_n^\lambda(z) J_{|m|} \left(2^{1/2} \zeta z^{1/2} \right) dz \right]^2 \right)^\alpha \quad (23b)$$

$$T_{\rho_{nm}}(\alpha) = \frac{1}{\alpha - 1} \left(1 - \frac{1}{(2\pi r_{eff}^2)^{\alpha-1}} \frac{1}{\alpha^{\alpha\lambda+1}} \left[\frac{n!}{\Gamma(n + \lambda + 1)} \right]^\alpha \right. \\ \left. \times \int_0^\infty e^{-z} z^{\alpha\lambda} \left[L_n^\lambda \left(\frac{z}{\alpha} \right)^2 \right]^\alpha dz \right) \quad (24a)$$

$$T_{\gamma_{nm}}(\alpha) = \frac{1}{\alpha - 1} \left[1 - \left(\frac{r_{eff}^2}{2\pi} \right)^{\alpha-1} \left[\frac{n!}{\Gamma(n + \lambda + 1)} \right]^\alpha \right. \\ \left. \times \int_0^\infty d\xi \xi \left(\left[\int_0^\infty e^{-z/2} z^{\lambda/2} L_n^\lambda(z) J_{|m|} \left(2^{1/2} \xi z^{1/2} \right) dz \right]^2 \right)^\alpha \right]. \quad (24b)$$

70 Similar to the Shannon case [2], the whole dependence of the Rényi position and momentum entropies
 71 on the uniform magnetic field B is embedded in the terms $\pm 2 \ln r_{eff}$. Concerning the Tsallis functionals,
 72 a dimensional incompatibility of the two items in Eqs. (24) precludes their direct application for
 73 the continuous probability distributions suggesting instead the forms presented in the corresponding
 74 uncertainty relation, Eq. (20), but below we will continue to write them keeping in mind that it is just a
 75 formal representation only.

For the ground band, $n = 0$, position components can be evaluated analytically:

$$R_{\rho_{0m}}(\alpha) = 2 \ln r_{eff} + \ln 2\pi + \frac{1}{1 - \alpha} \ln \frac{\Gamma(\alpha\lambda + 1)}{\alpha^{\alpha\lambda+1} \Gamma^\alpha(\lambda + 1)} \quad (25)$$

$$T_{\rho_{0m}}(\alpha) = \frac{1}{\alpha - 1} \left[1 - \frac{1}{(2\pi r_{eff}^2)^{\alpha-1}} \frac{\Gamma(\alpha\lambda + 1)}{\alpha^{\alpha\lambda+1} \Gamma^\alpha(\lambda + 1)} \right]. \quad (26)$$

76 Three limits of the last two dependencies are:
 for the Rényi entropy:

$$R_{\rho_{0m}}(\alpha) = 2 \ln r_{eff} + \ln 2\pi - \ln \alpha \\ - [\lambda(\gamma + \ln \alpha) + \ln(\alpha \Gamma(\lambda + 1))] \alpha + \dots, \quad \alpha \rightarrow 0 \quad (27a)$$

$$R_{\rho_{0m}}(\alpha) = S_{\rho_{0m}} + \frac{1}{2} \lambda \left[1 - \lambda \psi^{(1)}(\lambda) \right] (\alpha - 1) + \dots, \quad \alpha \rightarrow 1 \quad (27b)$$

$$R_{\rho_{0m}}(\alpha) = 2 \ln r_{eff} + \ln 2\pi + \lambda(1 - \ln \lambda) + \ln \Gamma(\lambda + 1) \\ + \frac{1}{\alpha} \left[\lambda(1 - \ln \lambda) + \ln \Gamma(\lambda + 1) + \frac{1}{2} \ln \frac{\alpha}{2\pi\lambda} \right] + \dots, \quad \alpha \rightarrow \infty, \quad (27c)$$

for the Tsallis entropy:

$$T_{\rho_{0m}}(\alpha) = \frac{2\pi r_{eff}^2}{\alpha} - 1 + \dots, \quad \alpha \rightarrow 0 \quad (28a)$$

$$T_{\rho_{0m}}(\alpha) = S_{\rho_{0m}} + c(r_{eff}, \lambda)(\alpha - 1) + \dots, \quad \alpha \rightarrow 1 \quad (28b)$$

$$T_{\rho_{0m}}(\alpha) = \frac{1}{\alpha} + \dots, \quad \alpha \rightarrow \infty, \quad (28c)$$

where the Shannon entropy $S_{\rho_{0m}}$ is [2]:

$$S_{\rho_{0m}} = 2 \ln r_{eff} + \ln 2\pi + \ln \Gamma(\lambda + 1) + \lambda [1 - \psi(\lambda)].$$

Here, $\psi(x) = d[\ln \Gamma(x)]/dx = \Gamma'(x)/\Gamma(x)$ and $\psi^{(n)}(x) = d^n \psi(x)/dx^n$, $n = 1, 2, \dots$, are psi (or digamma) and polygamma functions, respectively [16], and γ is Euler's constant. Also, $c(r_{eff}, \lambda)$ is a function containing a sum of several terms with miscellaneous products of different powers of $\ln r_{eff}$, λ , $\Gamma(\lambda)$, $\psi(\lambda)$ and $\psi^{(1)}(\lambda)$. Due to its unwieldy structure, we do not present its explicit form here. There are a few relevant points worth mentioning during the discussion of these equations. First, at the coefficient α approaching zero both position entropies diverge, Eqs. (27a) and (28a), since, as mentioned in the Introduction, the integration of the constant value over the (semi-)infinite interval essentially yields infinity. Invoking Taylor expansion of Eqs. (23a) and (24a) with respect to the small parameter α , it is easy to show that the logarithmic- and inverse-like divergences for the Rényi and Tsallis entropies, respectively, are characteristic at $\alpha \rightarrow 0$ for the arbitrary band with $n \geq 1$. Second, a comparison between Eqs. (27b) and (28b) reconfirms [31] that at the Rényi and Tsallis parameter tending to unity the corresponding entropies approach their Shannon counterpart along different paths. Next, as it follows, e.g., from Eq. (25), at the arbitrary coefficient α and $\phi_{AB} = 0$ the position Rényi entropy is an increasing function of the absolute value of the azimuthal index m . As our numerical results show, the same statement holds true for the radial quantum number n too. Also, the leading term of Eq. (27c) follows straightforwardly from the expression

$$R_{\rho, \gamma}(\infty) = -\ln \left(\frac{\rho_{max}}{\gamma_{max}} \right) \quad (29)$$

with the subscript in the right-hand side denoting a global maximum of the corresponding function. To find its location r_{max} for the position density, one needs to solve a polynomial equation

$$(\lambda - z)L_n^\lambda(z) - 2zL_{n-1}^{\lambda+1}(z) = 0, \quad n = 0, 1, \dots, \quad (30)$$

with $z = \frac{1}{2} \frac{r^2}{r_{eff}^2}$ what for the ground band reproduces the first line of Eq. (27c). For adjacent higher lying set of levels with $n = 1$ one has $z_{max} = \lambda + \frac{3}{2} - \frac{1}{2} \sqrt{8\lambda + 9}$ and:

$$R_{\rho_{1m}}(\infty) = 2 \ln r_{eff} + \ln 2\pi + \ln \Gamma(\lambda + 2) + z_{max} - \lambda \ln z_{max} - 2 \ln \frac{\sqrt{8\lambda + 9} - 3}{2}. \quad (31)$$

77 Finally, as a prerequisite to the analysis of the following subsection, let us underline that position
78 entropies are defined at any positive Rényi or Tsallis parameter.

79 2.2. Momentum components

For the singly connected geometry of the QD with $a = \nu = 0$ the expressions from Eqs. (25) and (26) simplify to

$$R_{\rho_{0m}}(\alpha)|_{a=\nu=0} = 2 \ln r_{eff} + \ln 2\pi + \frac{1}{1-\alpha} \ln \frac{\Gamma(|m|\alpha + 1)}{(|m|!)^\alpha \alpha^{|m|\alpha+1}} \quad (32)$$

$$T_{\rho_{0m}}(\alpha)|_{a=\nu=0} = \frac{1}{\alpha - 1} \left[1 - \frac{1}{(2\pi r_{eff}^2)^{\alpha-1}} \frac{\Gamma(|m|\alpha + 1)}{(|m|!)^\alpha \alpha^{|m|\alpha+1}} \right]. \quad (33)$$

At the same time, with the help of Eq. (10b) the momentum components are expressed analytically too:

$$R_{\gamma_{0m}}(\alpha)|_{a=v=0} = -2 \ln r_{eff} + \ln \frac{\pi}{2} + \frac{1}{1-\alpha} \ln \frac{\Gamma(|m|\alpha + 1)}{(|m|!)^\alpha \alpha^{|m|\alpha+1}} \quad (34)$$

$$T_{\gamma_{0m}}(\alpha)|_{a=v=0} = \frac{1}{\alpha-1} \left[1 - \left(\frac{2}{\pi} r_{eff}^2 \right)^{\alpha-1} \frac{\Gamma(|m|\alpha + 1)}{(|m|!)^\alpha \alpha^{|m|\alpha+1}} \right]. \quad (35)$$

80 Note that the dependencies of the position and momentum components of, e.g., the Rényi entropy on the
 81 coefficient α are, apart from the constant factor, the same what can be tracked back to the fact that the
 82 corresponding waveforms from Eqs. (10) present modified Gaussians. This also explains why the sum
 83 of the entropies from the corresponding uncertainty relation, Eq. (21), takes the same values at the Rényi
 84 parameters of one half and infinity, see Sec. 2.3.2.

Eqs. (32) – (35) manifest that under these special conditions of the 2D singly connected topology, the momentum entropies do exist at any non-negative coefficient α . However, situation changes drastically at $a + |\nu| \neq 0$ when the topology turns into the doubly connected one. To derive the lower limit of the semi-infinite range $[\alpha_{TH}, +\infty)$ where the momentum entropies exist, one needs to consider the inner integral in Eqs. (23b) and (24b) that, as stated before [2], does not have an analytic representation. Nevertheless, for our purpose it suffices to recall that the Laguerre polynomial $L_n^\lambda(z)$ of degree $n = 0, 1, 2, \dots$ is a linear combination of all powers of its argument z from zero to n . Accordingly, considering the integral

$$\int_0^\infty e^{-z/2} z^{\lambda/2+n'} J_{|m|} \left(2^{1/2} \zeta z^{1/2} \right) dz$$

with $n' = 0, \dots, n$, one finds [17,60] that it can be represented by the Kummer confluent hypergeometric function ${}_1F_1(a; b; x)$ [16,17] as

$$\begin{aligned} \int_0^\infty e^{-z/2} z^{\lambda/2+n'} J_{|m|} \left(2^{1/2} \zeta z^{1/2} \right) dz &= 2^{n'+1+\lambda/2} \frac{\Gamma \left(n' + 1 + \frac{\lambda+|m|}{2} \right)}{|m|!} \\ &\times \zeta^{|m|} {}_1F_1 \left(n' + 1 + \frac{\lambda+|m|}{2}; |m| + 1; -\zeta^2 \right). \end{aligned} \quad (36)$$

Note that for the AB-free QD the coefficient λ simplifies to $|m|$, and then for $n' = 0$ the Kummer function in Eq. (36) degenerates to the fading exponent with $\zeta \equiv r_{eff} k$ recovering in this way Eq. (10b), as expected. In general case, replacing Laguerre polynomial in Eqs. (23b) and (24b) by $z^{n'}$, calculating inner integral with the help of Eq. (36) and utilizing asymptotic properties of the confluent hypergeometric function [16], one finds that the outer integrals in just mentioned equations will converge [59] at $\alpha > 1/(2 + \lambda + n')$. Consequently, the upper limit of the right-hand side of this inequality, which is achieved at the smallest power of the argument of the Laguerre polynomial, $n' = 0$, will determine a global range of convergence of the momentum entropies R_γ and T_γ , and the threshold value is:

$$\alpha_{TH} = \begin{cases} 0, & a = v = 0 \\ \frac{1}{2+\lambda}, & a + |\nu| \neq 0. \end{cases} \quad (37)$$

85 Remarkably, this range is not influenced by the uniform field B being, on the other hand, a function of the
 86 potential profile, as asserted before for the 1D structures [31]. Observe that Eq. (37) contains the parameter
 87 a defining the inner steepness of $U(r)$ but not the outer confinement that is characterized by ω_0 . Also, α_{TH}
 88 strongly depends on the orbital itself or, more specifically, on its azimuthal quantum number m , which

89 determines the distance from the centre of the ring. In addition, recalling the definition of the parameter λ
 90 from Eq. (7d), one can use the AB flux as a switch that triggers the existence of the momentum entropies.

Next, using Eq. (29) and the fact that for the angle-independent waveforms, $m = 0$, their global maxima are achieved at the zero momentum, $k = 0$, as can be easily shown from Eq. (6b), one calculates the corresponding densities as [60]

$$\gamma_{n0}(\mathbf{0}) = r_{eff}^2 \frac{2^{\lambda+1}}{\pi} \frac{n!}{\Gamma(n+\lambda+1)} \frac{\Gamma^2\left(\left[\frac{n}{2}\right] + 1 + \frac{\lambda}{2}\right)}{\left(\left[\frac{n}{2}\right]!\right)^2} \quad (38)$$

with $[x]$ denoting an integer part of x , what leads to the entropies:

$$R_{\gamma_{n0}}(\infty) = -2 \ln r_{eff} + \ln \frac{\pi}{2} - \ln \left(2^\lambda \frac{n!}{\Gamma(n+\lambda+1)} \frac{\Gamma^2\left(\left[\frac{n}{2}\right] + 1 + \frac{\lambda}{2}\right)}{\left(\left[\frac{n}{2}\right]!\right)^2} \right). \quad (39)$$

91 Note that for the AB-free QD, $a = \nu = 0$, when λ in Eq. (39) turns to zero, it is consistent at $n = 0$ with
 92 the limit $\alpha \rightarrow \infty$ of Eq. (34), as expected.

93 2.3. Uncertainty relations

94 Besides playing a fundamental role in the quantum foundations, entropic uncertainty relations
 95 find miscellaneous applications in information theory, ranging from entanglement witnessing to
 96 wave-particle duality to quantum cryptography etc. [61,62] Below, Tsallis and Rényi inequalities are
 97 considered separately but their common features, such as a saturation to identity, are underlined.

98 2.3.1. Tsallis entropy

For the ground band, $n = 0$, of the singly connected topology of the QD, $a = \nu = 0$, Tsallis inequality from Eq. (20) with the help of the dependencies from Eqs. (33) and (35) is converted to

$$\left(2^{1/2} r_{eff}\right)^{\frac{1-\alpha}{\alpha}} \frac{\Gamma^{\frac{1}{2\alpha}}(|m|\alpha + 1)}{\alpha^{|m|/2} (\pi|m|!)^{1/2}} \geq \left(2^{1/2} r_{eff}\right)^{\frac{\beta-1}{\beta}} \frac{\Gamma^{\frac{1}{2\beta}}(|m|\beta + 1)}{\beta^{|m|/2} (\pi|m|!)^{1/2}}, \quad (40)$$

where the coefficients α and β are conjugated by Eq. (18). Obviously, due to this, Eq. (40) is dimensionally correct, as

$$\frac{1-\alpha}{\alpha} = \frac{\beta-1}{\beta}. \quad (41)$$

Note that for the lowest energy orbital of this configuration, $m = 0$, Eq. (40) turns into the identity at any Tsallis parameter α without the restriction from Eq. (19) what is explained by the fact that its both position and momentum probability distributions are Gaussian functions, which play a very special role for the entropic inequalities in quantum information [63]. Next, as already mentioned in the Introduction, at any other azimuthal index m the relation from Eq. (40) turns into the equality at $\alpha = \beta = 1$ around which its dimensionless part (without the coefficient r_{eff}) becomes

$$\frac{1 + (-\ln 2 - \ln(|m|!) - |m| [1 - \psi(|m| + 1)]) (\alpha - 1)}{\pi^{1/2}} \geq \frac{1 + (-\ln 2 + \ln(|m|!) + |m| [1 - \psi(|m| + 1)]) (\alpha - 1)}{\pi^{1/2}}, \quad \alpha \rightarrow 1, \quad (42)$$

and since, as it follows from the properties of the psi function [16],

$$\ln(|m|!) + |m| [1 - \psi(|m| + 1)] > 0, \quad |m| \geq 1, \quad (43)$$

the inequality from Eq. (42) holds to the left of $\alpha = 1$ only, in accordance with the general Sobolev rule, Eq. (19). At the opposite side of this interval, the Tsallis relation simplifies to

$$r_{eff} \left(\frac{2}{\pi |m|!} \right)^{1/2} 2^{|m|/2} \Gamma \left(\frac{|m|}{2} + 1 \right) \geq r_{eff} \left(\frac{2}{\pi |m|!} \right)^{1/2} \left(\frac{|m|}{e} \right)^{|m|/2}, \quad \alpha \rightarrow \frac{1}{2}, \quad (44)$$

99 where we have retained the leading terms only in the Taylor expansion of both sides of Eq. (40) around
 100 $\alpha = 1/2$. The gap between the left and right sides of this inequality widens as the index $|m|$ increases.
 101 Also, at the extremely large Tsallis parameter, $\alpha \rightarrow \infty$, the dimensionless parts exchange their places and
 102 simultaneously are divided by two as compared to Eq. (44).

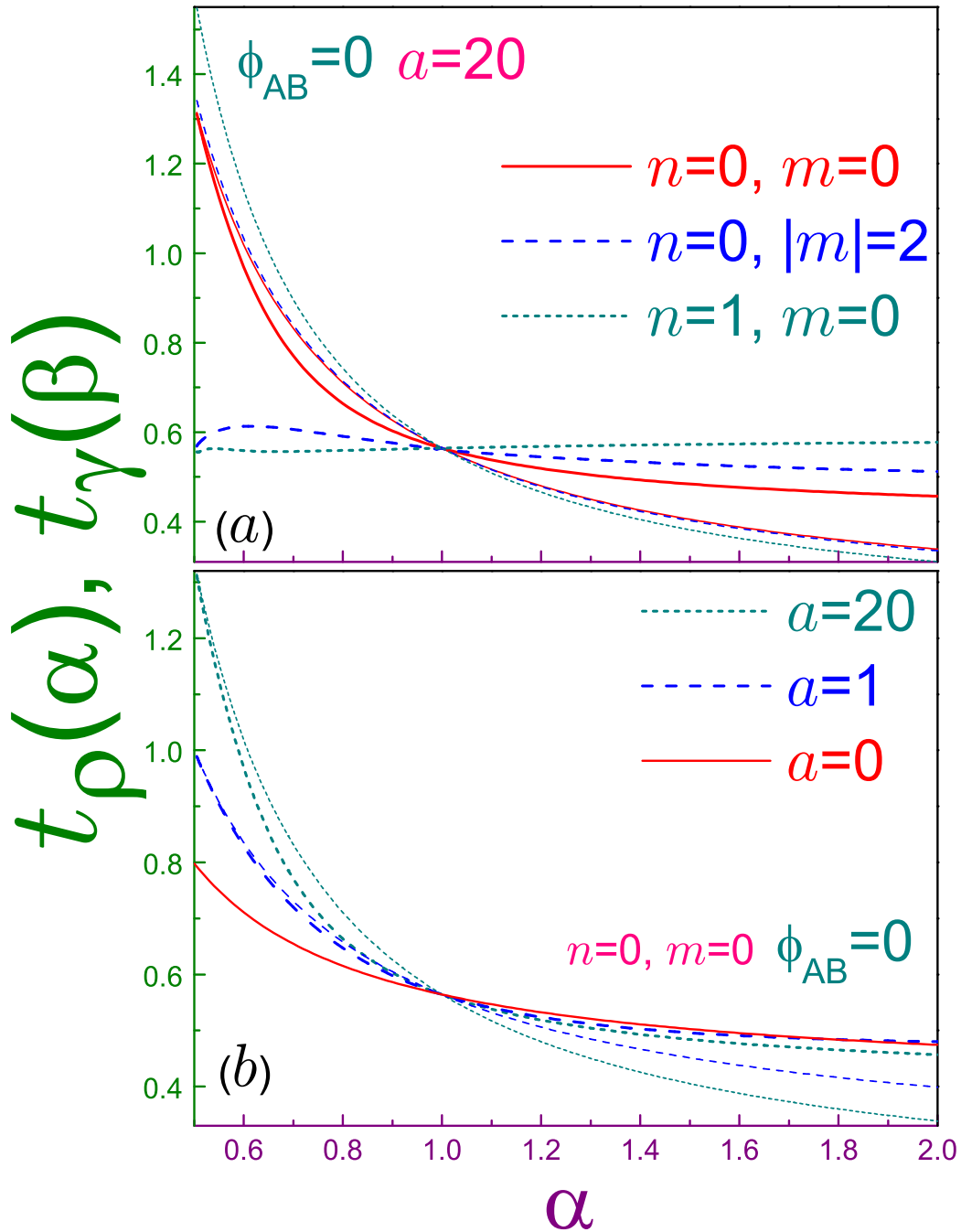


Figure 1. Dimensionless left (thin lines) $t_{\rho_{nm}}(\alpha)$, Eq. (46a), and right (thick curves) $t_{\gamma_{nm}}(\beta)$, Eq. (46b), sides of the Tsallis uncertainty relation, Eq. (20), as functions of coefficient α where in panel (a) the parameter a is equal to 20 with solid lines showing the $n = m = 0$ state, dashed curves are for the $n = 0, |m| = 2$ level and dotted lines stand for $n = 1, m = 0$ state whereas window (b) depicts the dependencies for several antidot strengths a of the $n = m = 0$ orbital: solid line is for the QD geometry ($a = 0$), dashed curves are for $a = 1$ and dotted functions are for $a = 20$. Note that vertical ranges in parts (a) and (b) are slightly different. For both panels, the AB flux is zero.

Turning to the discussion of the general geometry of the doubly connected topology, $a + |\nu| > 0$, let us note first that since here the radius r_{eff} enters either side in the same way as for the QD, Eq. (40), the

Tsallis inequality at any coefficient α does *not* depend on the uniform magnetic field \mathbf{B} , as was the case for the Shannon regime too [2]. Next, observe that at $\alpha = 1/2$ the left-hand side of the general Tsallis inequality, Eq. (20), becomes:

$$\frac{1}{2\pi} \int_{\mathbb{R}^2} |\Psi_{nm}(\mathbf{r})| d\mathbf{r}. \quad (45)$$

For the rotationally symmetric orbital [when the function $\Psi_{n0}(\mathbf{r})$ is real] of the lowest band [when the radial component $R_{0m}(r)$ preserves its sign along the r axis], this expression reduces to $\Phi_{00}(\mathbf{0})$, see Eq. (4a). On the other hand, in the same limit (i.e., at $\beta = \infty$) the right-hand sides of Eqs. (20) and (17) turn to

$$|\Phi_{nm}(\mathbf{k})|_{max}.$$

As already mentioned in Sec. 2.2, for the angle-independent, $m = 0$, momentum functions their global maximum is located at the zero wave vector. Hence, we have shown that the $n = m = 0$ orbital at $\alpha = 1/2$ transforms the Tsallis inequality into the identity. Existence of such a level was conjectured before [31] when it was stated, however, that it has to be the lowest-energy state. But the well-known property of the QR is the fact that the increasing magnetic field \mathbf{B} causes consecutive crossings of the energies of the same band orbitals with adjacent non-positive azimuthal indices [6,7,11,13]; for example, the $n = m = 0$ level exhibits the lowest energy only in the range of the cyclotron frequencies from zero to [13]

$$2^{1/2} \frac{(a+1)^{1/2} - a^{1/2}}{([a(a+1)]^{1/2} - a)^{1/2}} \omega_0,$$

after which it lies above the $n = 0, m = -1$ state. Accordingly, the previous conjecture [31] stays correct in a sense that there is the only orbital that at $\alpha = 1/2$ does saturate the Tsallis uncertainty relation; however, it is not necessarily the lowest-energy level (at least, for the 2D structures in the magnetic field). Solid lines in panel (a) of Fig. 1 that depicts quantities

$$t_\rho(\alpha) = r_{eff}^{\frac{\alpha-1}{\alpha}} \left(\frac{\alpha}{\pi} [1 + (1-\alpha)T_\rho(\alpha)] \right)^{1/(2\alpha)} \quad (46a)$$

$$t_\gamma(\beta) = r_{eff}^{\frac{1-\beta}{\beta}} \left(\frac{\beta}{\pi} [1 + (1-\beta)T_\gamma(\beta)] \right)^{1/(2\beta)}, \quad (46b)$$

which are dimensionless left and right parts, respectively, of Eq. (20), emphasize the saturation by $n = m = 0$ quantum state of the corresponding uncertainty not only at $\alpha = 1$, as all other orbitals do (see dashed and dotted curves), but at the Tsallis coefficient being equal to one half too. Window (b) compares the influence of the width of the ring on the interrelation between position and momentum Tsallis parts of this orbital: it is seen that for the thinner ring (greater a [2,13]) the difference between them increases in the interval from Eq. (19). The dependencies shown in this figure as well as in Fig. 2 are universal in a sense that they do not depend on the uniform magnetic field. For completeness, we also provide the analytic expression of the left-hand side of the Tsallis inequality for the ground band, $n = 0$:

$$\left(2^{1/2} r_{eff} \right)^{\frac{1-\alpha}{\alpha}} \frac{\Gamma^{\frac{1}{2\alpha}}(\lambda\alpha + 1)}{\pi^{1/2} \alpha^{\lambda/2} \Gamma^{\frac{1}{2}}(\lambda + 1)}, \quad (47)$$

103 which generalizes its QD counterpart from Eq. (40).

104 2.3.2. Rényi entropy

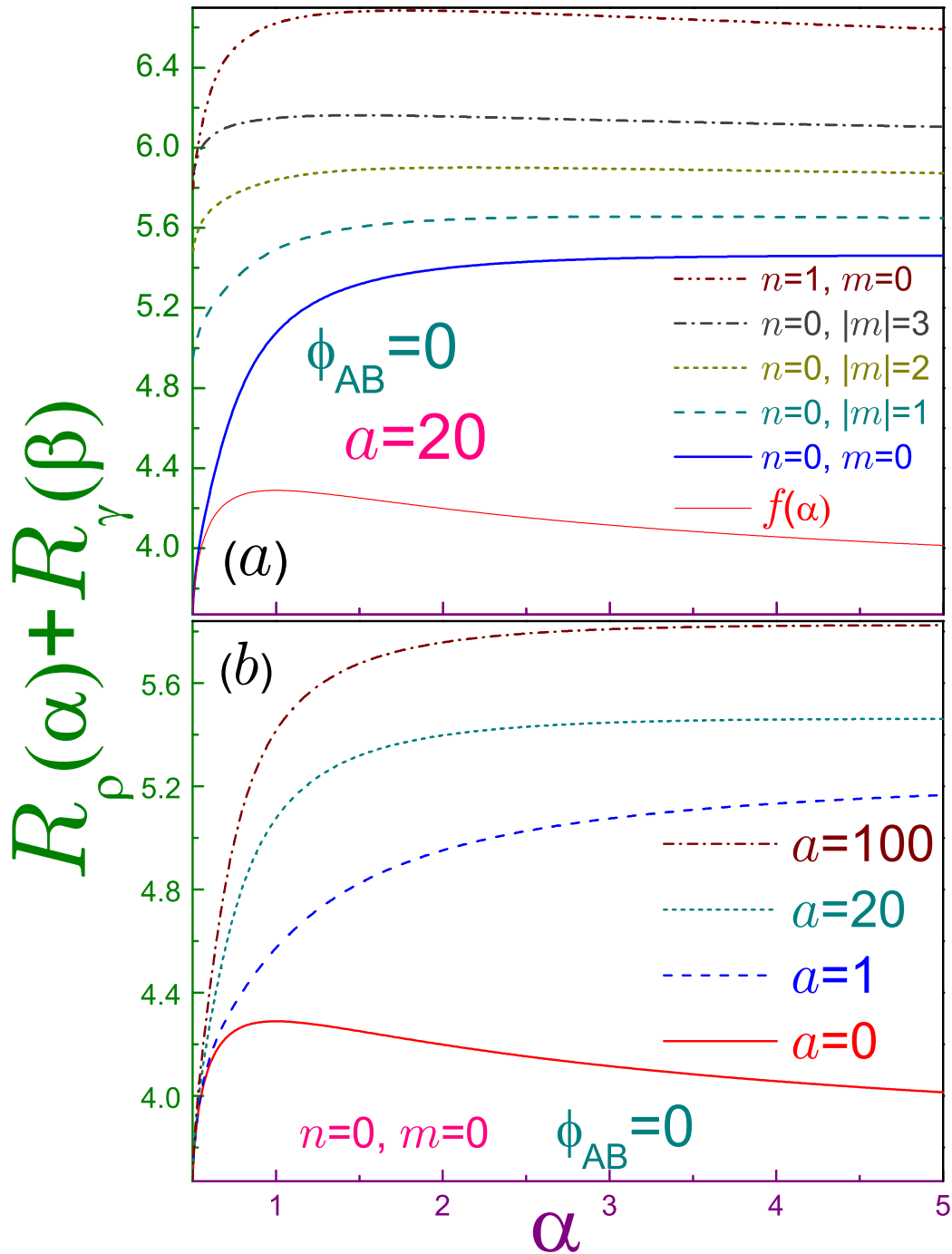


Figure 2. Sum of the position and momentum Rényi entropies $R_{\rho_{nm}}(\alpha) + R_{\gamma_{nm}}(\beta)$ as function of parameter α where in panel (a) the dependencies at the fixed antidot strength $a = 20$ are shown for several indices n and m whereas in (b) the $n = m = 0$ orbital is depicted at different a . In panel (a), thick solid line is for $n = m = 0$ level, dotted curve - for $n = 0, |m| = 1$ state, dashed one stands for $n = 0, |m| = 2$ orbital, dash-dotted line - $n = 0, |m| = 3$ case, and dash-dot-dotted dependence describes $n = 1, m = 0$ level with thin solid curve representing function $f(\alpha)$ from Eq. (48), which is the right-hand side of the Rényi uncertainty relation, Eq. (21). The latter dependence is also reproduced by the solid line in panel (b) where dashed curve is for $a = 1$, dotted one - for $a = 20$ [corresponding to thick solid line in panel (a)], and dash-dotted curve is for $a = 100$. For both windows, the AB intensity is zero, $\phi_{AB} = 0$, and their upper vertical limits differ from each other.

105 As it follows from Eqs. (23), the uncertainty relation, Eq. (21), is not affected by the uniform magnetic
 106 field. This statement, similar to its Tsallis counterpart from the previous subsection, expands to any Rényi
 107 parameter a previous conclusion for the Shannon entropies [2].

108 Eqs. (32) and (34) with $m = 0$ directly show that the AB-free QD lowest-energy orbital saturates the
 109 entropic inequality at the arbitrary coefficient α . Explanation of this is the same as for the Tsallis entropy,
 110 see Sec. 2.3.1.

For $l = 2$, right-hand side of inequality (21), which we will denote as

$$f(\alpha) = 2 \left[\ln \pi - \ln \alpha + \frac{\alpha - 1/2}{\alpha - 1} \ln(2\alpha - 1) \right], \quad (48)$$

reaches its only maximum of $2(1 + \ln \pi) = 4.2894 \dots$ at the Shannon regime, $\alpha = 1$, and approaches
 $2 \ln 2\pi = 3.6757 \dots$ at $\alpha \rightarrow 1/2$ and $\alpha \rightarrow \infty$ [31]. For the arbitrary m , the same limits of the sum $R_{\rho_{0m}}(\alpha) +$
 $R_{\gamma_{0m}}(\beta)$ at $a = \nu = 0$ are:

$$2 \ln 2\pi + |m|(1 + \ln 2) + \ln \frac{\Gamma^2\left(\frac{|m|}{2} + 1\right)}{|m|^{|m|}} - 2 \left(\alpha - \frac{1}{2} \right) \ln \left(\alpha - \frac{1}{2} \right) + \dots, \quad \alpha \rightarrow \frac{1}{2} \quad (49a)$$

$$2(1 + \ln \pi + \ln(|m|!) + |m| [1 - \psi(|m| + 1)]) - \left[\frac{1}{3} + \frac{1}{3}|m|^3 \psi(2, |m| + 1) + |m|^2 \psi(1, |m| + 1) - \frac{2}{3}|m| \right] (\alpha - 1)^2 + \dots, \quad \alpha \rightarrow 1 \quad (49b)$$

$$2 \ln 2\pi + |m|(1 + \ln 2) + \ln \frac{\Gamma^2\left(\frac{|m|}{2} + 1\right)}{|m|^{|m|}} + \frac{1}{2} \frac{\ln \alpha}{\alpha} + \dots, \quad \alpha \rightarrow \infty. \quad (49c)$$

111 Note that, as it follows from Eqs. (49a) and (49c), the sum of the entropies of the generalized Gaussian
 112 approaches its edge values (which are equal to each other due to the fact that each item in it has the
 113 same dependence on the Rényi parameter and, as a result, due to the condition from Eq. (18), at the rims
 114 α and β simply interchange their places) from above and since the expression in the square brackets in
 115 Eq. (49b) is always positive, left-hand side of Eq. (21) reaches its maximum at the Shannon entropy. Also,
 116 the leading terms in all three cases are increasing functions of the magnetic index what means that at
 117 the greater $|m|$ the corresponding curve lies higher satisfying, of course, the uncertainty relation. As our
 118 numerical results show, the same statement holds true at the fixed quantum number m and the increasing
 119 principal index n .

120 For the QR, $a > 0$, a comparison of Eqs. (25), (39) and (48) proves that the $n = m = 0$ orbital does
 121 convert at $\alpha = 1/2$ the Rényi uncertainty into the identity, as it did for the Tsallis inequality too. This is
 122 also exemplified in Fig. 2(a), which shows that its sum $R_{\rho}(\alpha) + R_{\gamma}(\beta)$ at any parameter α is the smallest
 123 one as compared to other levels. Dependence of the left-hand side of Eq. (21) on n and $|m|$ is the same
 124 as for the QD described in the previous paragraph. Contrary to Eqs. (49a) and (49c), for the doubly
 125 connected topology the sum approaches different limits at the Rényi parameters one half and infinity.
 126 Location of the only (relatively broad, as compared to the QD) maximum of $R_{\rho_{nm}}(\alpha) + R_{\gamma_{nm}}(\beta)$ is now
 127 n and $|m|$ dependent: as panel (a) demonstrates, it is shifted to smaller α at the greater $|m|$ and n . The
 128 same effect is achieved by thinning the ring, as depicted in window (b) of Fig. 2 where also it is shown
 129 that the sum gets larger for the increasing antidot strength. In addition, it is seen that the transformation
 130 of the uncertainty relation for the $n = m = 0$ state into the identity at $\alpha = 1/2$ is independent from the
 131 nonzero a , as it follows from Eqs. (25) and (39). Finally, the remark about the conjecture [31] discussed for
 132 the Tsallis entropies in Sec. 2.3.1, directly applies to their Rényi counterparts too.

133 3. AB Rényi entropy

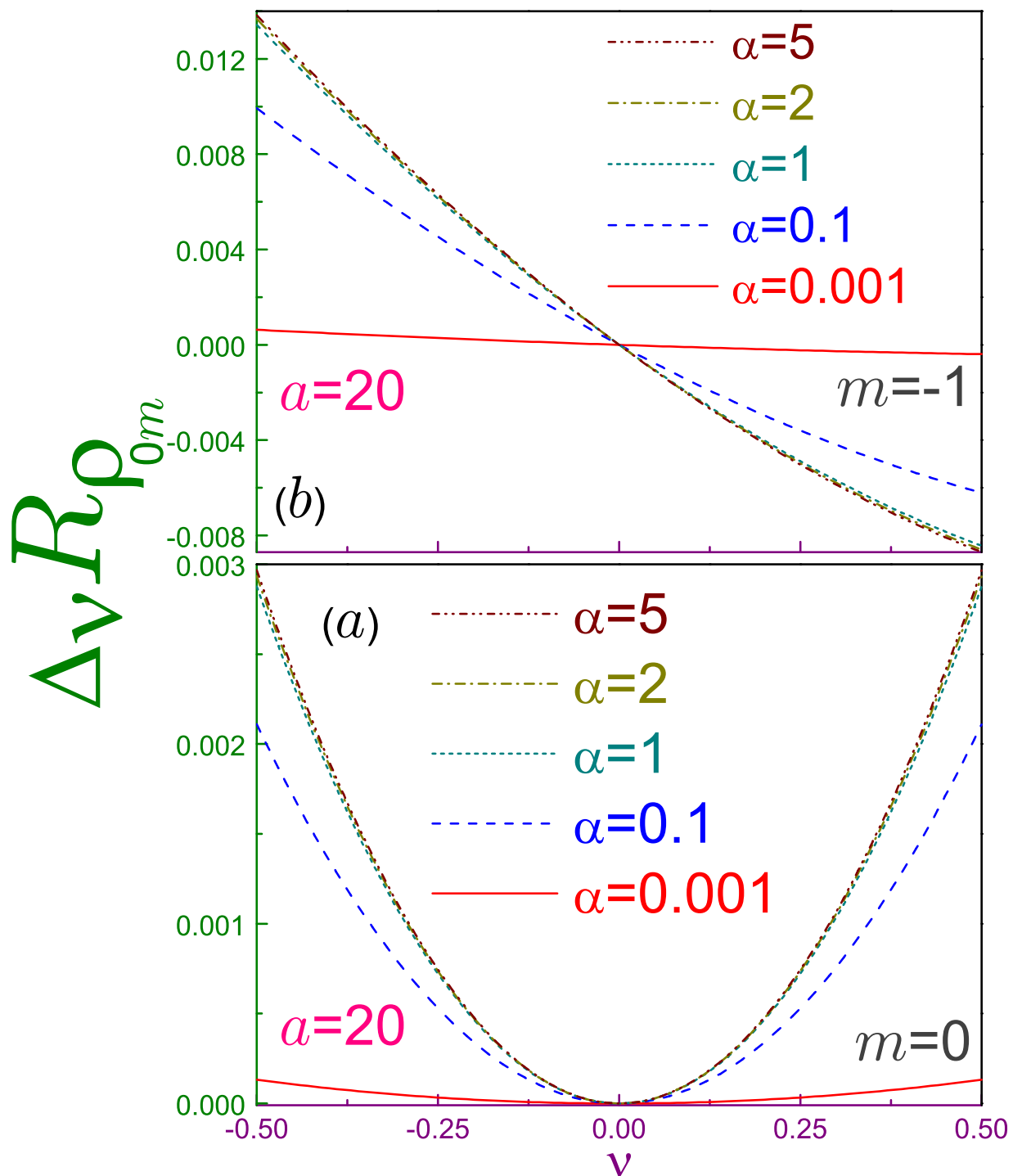


Figure 3. Difference $\Delta v R_{\rho_{0m}}$, Eq. (53), at $a = 20, B = 0, r_0 = 1$ and (a) $m = 0$ and (b) $m = -1$ where solid lines are for the Rényi parameter being equal to 0.001, dashed curves are for $\alpha = 0.1$, dotted ones – for $\alpha = 1$, dashed-dotted lines – for $\alpha = 2$, and dash-dot-dotted curves depict the dependence at $\alpha = 5$.

Due to the dimensional incompatibility for the continuous distributions of the two items in the right-hand sides of Eqs. (14), we do not discuss dependencies of the Tsallis measures on ϕ_{AB} . To describe a variation of the position Rényi entropy $R_{\rho_{00}}(\alpha)$ with the AB flux, one has to calculate Taylor expansion of Eq. (25) with respect to the parameter ν and to truncate the series at the first nonvanishing power of the AB intensity:

$$R_{\rho_{00}}(\nu; \alpha) = 2 \ln r_{eff} + \ln 2\pi + \frac{1}{\alpha - 1} \left[\left(a^{1/2} \alpha + 1 \right) \ln \alpha + \ln \frac{\Gamma^\alpha \left(a^{1/2} + 1 \right)}{\Gamma \left(a^{1/2} \alpha + 1 \right)} \right] + \frac{\alpha}{2a^{1/2}(\alpha - 1)} \left[\psi \left(a^{1/2} + 1 \right) - \psi \left(a^{1/2} \alpha + 1 \right) + \ln \alpha \right] \nu^2. \quad (50)$$

Properties of digamma function [16] applied to the analysis of the term at ν^2 reveal that the entropy $R_{\rho_{00}}$ at the arbitrary Rényi parameter and the width of the ring is, similar to the zero-uniform-field energy

$$E_{n0}(a, \nu; 0) = \hbar \omega_0 \left(2n + 1 + \frac{1}{2a^{1/2}} \nu^2 \right), \quad (51)$$

a convex function of the flux and since the persistent current is expressed with the help of the derivative of the energy with respect to ν , Eq. (12), the position entropy can be used for evaluating J_{nm} too. A steepness $\partial R_{\rho_{nm}}(\nu; \alpha) / \partial \nu$ of the $R_\rho - \nu$ characteristics is strongly α - and a -dependent as, for example, three important limits show:

$$R_{\rho_{00}}(\nu; \alpha) = 2 \ln r_{eff} + \ln 2\pi - \ln \alpha - \left[a^{1/2} (\gamma + \ln \alpha) + \ln \left(\alpha \Gamma \left(a^{1/2} + 1 \right) \right) \right] \alpha - \frac{1}{2a^{1/2}} \left[\gamma + \psi \left(a^{1/2} + 1 \right) + \ln \alpha \right] \alpha \nu^2, \quad \alpha \rightarrow 0 \quad (52a)$$

$$R_{\rho_{00}}(\nu; \alpha) = 2 \ln r_{eff} + \ln 2\pi + \ln \Gamma \left(a^{1/2} + 1 \right) + a^{1/2} \left[1 - \psi \left(a^{1/2} \right) \right] + \frac{1}{2} a^{1/2} \left[1 - a^{1/2} \psi^{(1)} \left(a^{1/2} \right) \right] (\alpha - 1) + \frac{1}{2} \left[\frac{1}{a^{1/2}} - \psi^{(1)} \left(a^{1/2} + 1 \right) \right] \nu^2 + \left[\frac{1}{2} + \frac{3}{a^{1/2}} + a \psi^{(2)} \left(a^{1/2} \right) - a^{1/2} \psi^{(1)} \left(a^{1/2} \right) \right] \frac{\alpha - 1}{a^{1/2}} \nu^2, \quad \alpha \rightarrow 1 \quad (52b)$$

$$R_{\rho_{00}}(\nu; \alpha) = 2 \ln r_{eff} + \ln 2\pi + a^{1/2} \left(1 - \ln a^{1/2} \right) + \ln \Gamma \left(a^{1/2} + 1 \right) + \frac{1}{\alpha} \left[a^{1/2} \left(1 - \ln a^{1/2} \right) + \ln \Gamma \left(a^{1/2} + 1 \right) + \frac{1}{2} \ln \frac{\alpha}{2\pi a^{1/2}} \right] + \frac{\psi \left(a^{1/2} + 1 \right) - \ln a^{1/2}}{2a^{1/2}} \nu^2 + \left[\frac{1}{2a^{1/2}} + \psi \left(a^{1/2} \right) - \ln a^{1/2} \right] \frac{\nu^2}{\alpha}, \quad \alpha \rightarrow \infty. \quad (52c)$$

First, let us point out that at $\alpha = 1$ the Rényi entropy, Eq. (52b), turns into its Shannon counterpart [2]², as expected. Second, dying coefficient α leads not only to the logarithmic divergence of the entropy but simultaneously suppresses its dependence on the AB field, as Eq. (52a) demonstrates. To exemplify a

² Eq. (38) in Ref. [2] contains two typos: first, the free item "+1" on the upper line of its right-hand side should be dropped and, second, the argument of the function $\psi^{(1)}$ on the third line should be $a^{1/2}$ instead of a . Also, the item $\frac{1}{2}$ on the first line of Eq. (40) there should enter with the negative sign. These typos do not affect any other results presented in that paper.

variation of the speed of change of the entropy with the flux $\partial R_{\rho_{00}}/\partial v$ at different Rényi coefficients, Fig. 3(a) depicts the quantity

$$\Delta_v R_{\rho_{nm}} = R_{\rho_{nm}}(v; \alpha) - R_{\rho_{nm}}(0; \alpha) \quad (53)$$

at $a = 20$ for $n = m = 0$. It is seen that as the parameter α decreases to the extremely small values (eventually reaching zero), the entropy loses its dependence on the flux (eventually becoming completely flat). This has a clear physical explanation; namely, at the vanishing α the integrand in Eq. (13a) degenerates to unity, which is not affected by the variation of the AB field. Increasing Rényi coefficient makes the slope steeper and at $\alpha \gtrsim 1$ the $R_\rho - v$ curve practically does not depend on α , as a comparison of the dotted, dash-dotted and dash-dot-dotted lines in the figure reveals. This slope saturation can be also deduced from the analysis of the corresponding terms

$$\frac{1}{2} \left[\frac{1}{a^{1/2}} - \psi^{(1)}(a^{1/2} + 1) \right]$$

and

$$\frac{\psi(a^{1/2} + 1) - \ln a^{1/2}}{2a^{1/2}}$$

134 at v^2 in Eqs. (52b) and (52c), respectively: they almost do not differ from each other, especially at the
 135 moderate and large a . Let us also point out that the convexity of the Rényi entropy and the relation
 136 between $R_{\rho, \gamma}$ and Onicescu energy, Eq. (16), explains the concavity of the position component of the
 137 latter [2].

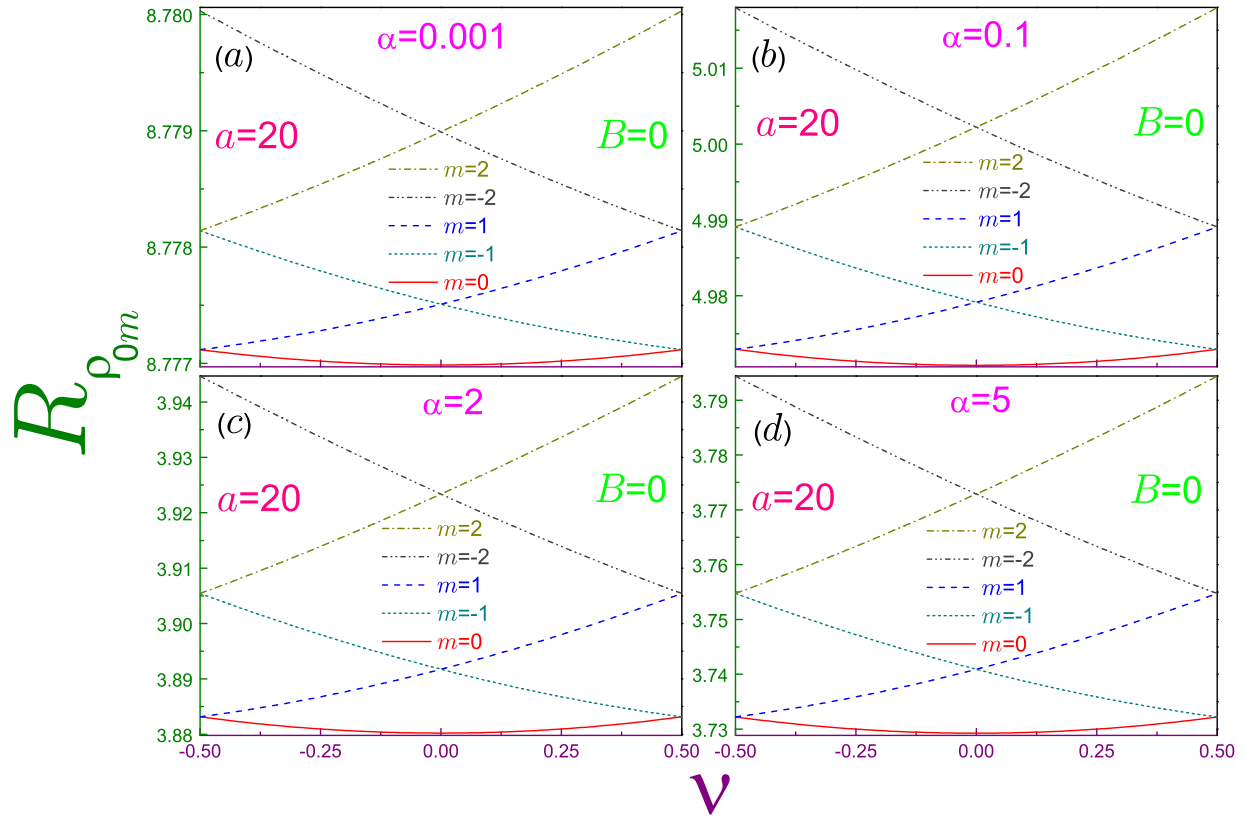


Figure 4. Position Rényi entropies $R_{\rho_{0m}}$ as functions of the normalized AB flux ν at $a = 20$, zero magnetic field and several parameters α where panel (a) is for $\alpha = 0.001$, window (b) - for $\alpha = 0.1$, subplot (c) is for $\alpha = 2$ and panel (d) shows the entropies at $\alpha = 5$. In each of the windows, solid curve denotes the orbital with $m = 0$, dotted line is for the level with $m = -1$, dashed line - $m = 1$, dash-dotted line describes the entropy of the state with $m = -2$, and dash-dot-dotted curve - with $m = 2$. Radius r_0 is assumed to be equal to unity. Note different scales and ranges of the vertical axis in each of the panels.

Fig. 4 shows $R_{\rho_{0m}} - \nu$ characteristics for three smallest $|m|$ and several Rényi parameters. Corresponding analysis of the Shannon dependencies revealed a strong similarity between $R_{\rho}(\nu; 1)$ and the energy spectrum [2]. This resemblance survives qualitatively at the arbitrary coefficient $\alpha \neq 1$; in particular, relations

$$R_{\rho_{nm}}\left(-\frac{1}{2}; \alpha\right) = R_{\rho_{n,-m+1}}\left(-\frac{1}{2}; \alpha\right) \quad (54a)$$

$$R_{\rho_{nm}}\left(\frac{1}{2}; \alpha\right) = R_{\rho_{n,-m-1}}\left(\frac{1}{2}; \alpha\right), \quad (54b)$$

which are elementary derived from Eq. (23a), are an exact replica of the corresponding degeneracy of the energy spectrum in the zero uniform magnetic field [2]. This is a consequence of the invariance of the radial part of the position waveform, Eq. (6a), energy, Eq. (11), and persistent current, Eq. (12), under the transformation

$$m \rightarrow m - 1, \quad \nu \rightarrow \nu + 1. \quad (55)$$

138 Also, at any α the slope retains the same sign as the azimuthal index m . Quantitatively, the magnitude of
139 the steepness $|\partial R_{\rho_{nm}} / \partial \nu|$ for any orbital, similar to the $n = m = 0$ state, decreases as the Rényi coefficient

140 tends to the progressively smaller values eventually becoming perfectly flat at $\alpha = 0$ whereas at $\alpha \gtrsim 1$
141 it is almost not affected by the variation of this parameter. Fig. 3(b) shows both these features for the
142 $n = 0, m = -1$ level. One can say that the decreasing Rényi factor increases the density of the position
143 components with its lowest threshold moving higher and in the opposite regime of the huge α the number
144 of the position Rényi entropies per unit interval saturates with its bottom being determined by the antidot
145 strength a .

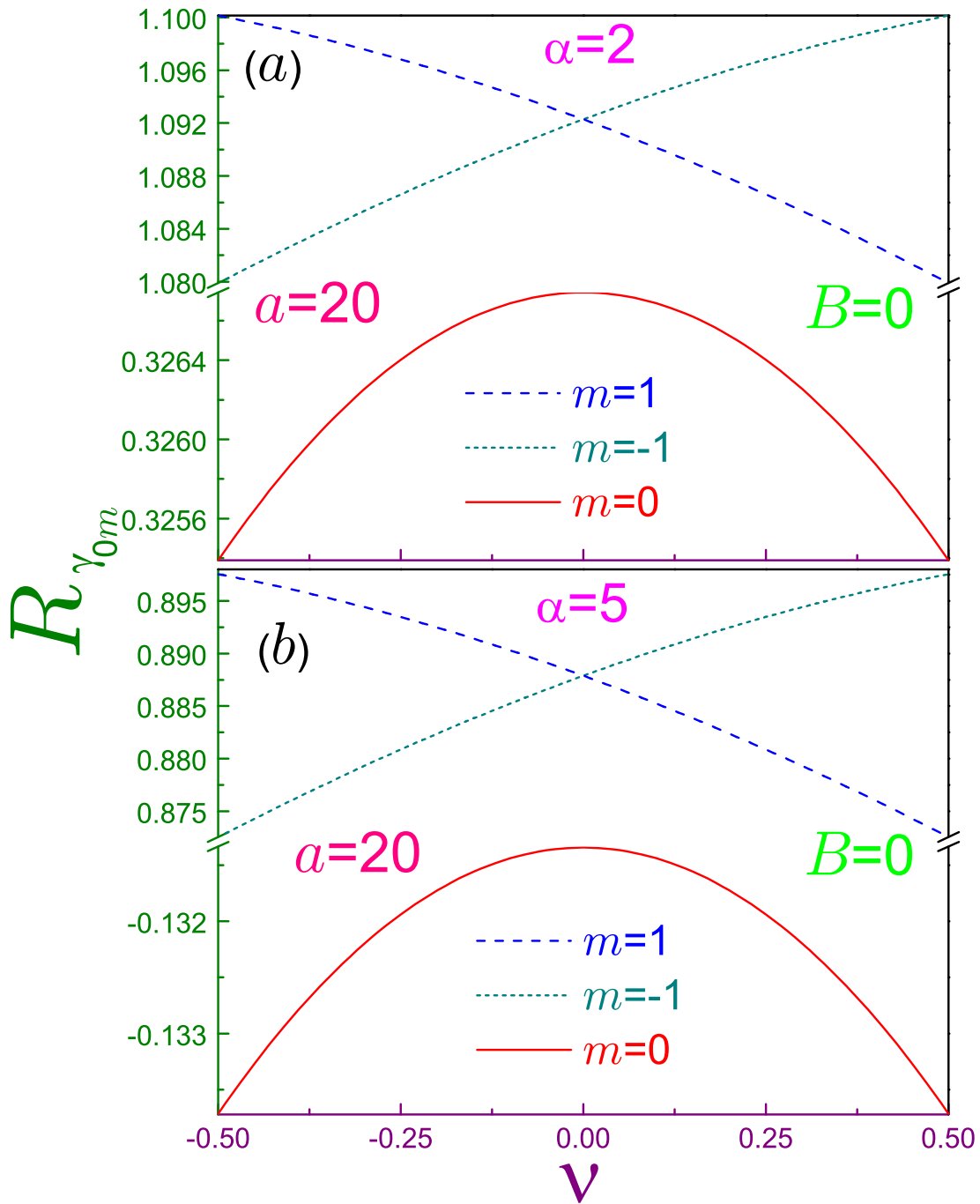


Figure 5. Momentum Rényi entropies $R_{\gamma_{0m}}$ for $m = 0$ and ± 1 as functions of the normalized AB flux ν for (a) $\alpha = 2$ and (b) $\alpha = 5$. All other parameters and conventions are the same as in Fig. 4. Due to the relatively small change of the entropies as compared to the distance between $R_{\gamma_{00}}$ and $R_{\gamma_{0,\pm 1}}$, vertical axes breaks have been inserted in panel (a) from 0.3267 to 1.0799 and in window (b) from -0.13133 to 0.8726. Note also different scales above and below the break in subplot (b).

146 Discussing momentum entropies dependence on the AB field, one has to recall that there is a lower
 147 nonzero threshold at which $R_{\gamma_{nm}}$ can be calculated. Eq. (37) reveals that if the momentum component, e.g.,
 148 for the rotationally symmetric orbitals, $m = 0$, takes finite value at the zero flux, it will stay bounded at

149 any arbitrary ϕ_{AB} . However, the opposite is not always true: a decreasing AB intensity increases for these
 150 levels α_{TH} what can lead to the divergence of the corresponding entropy at the fixed Rényi coefficient. For
 151 $m \neq 0$ states the symmetry with respect to the sign of the flux is lost; accordingly, the entropy that was
 152 finite at some particular α and zero AB field can become infinite with the variation of the flux. Thus, as
 153 mentioned in Sec. 2.2, the AB intensity can switch the existence of the momentum functionals.

154 Numerical analysis shows that momentum components $R_{\gamma_{nm}}$, contrary to their position counterparts,
 155 are concave functions of the flux. A particular case of this statement for the Shannon entropy, $\alpha = 1$, was
 156 established before [2] and is generalized here to all other values of the Rényi coefficient. Fig. 5 exemplifies
 157 the entropy behavior at the two parameters α . Steepness $|\partial R_{\gamma_{nm}}/\partial \nu|$ becomes more precipitous for the
 158 larger α , as was the case for $R_{\rho_{nm}}$ too. It is observed that for the same orbital the sign of the slope of the
 159 momentum Rényi functional is just the opposite to its position fellow. The relations similar to Eqs. (54) do
 160 not exist for $R_{\gamma_{nm}}$ what is a direct consequence of the expression for the corresponding radial waveform,
 161 Eq. (6b). The gap between the entropies with different $|m|$ gets wider as the Rényi factor grows whereas
 162 the range of change of each $R_{\gamma_{nm}}$ at $\alpha \gtrsim 1$ stays almost unchanged. This is the reason the vertical breaks
 163 have been introduced in Fig. 5.

164 As a last note of this discussion, let us mention that, similar to the Shannon case [2], the background
 165 uniform magnetic field, $B \neq 0$, does not change the shape of the $R_{\rho,\gamma} - \phi_{AB}$ characteristics but simply
 166 shifts them in the vertical direction, as it follows, for instance, from Eq. (50). Accordingly, Eqs. (54)
 167 representing the invariance under the transformation from Eq. (55) stay intact too. A structure of the
 168 energy spectrum in this case is analyzed in Ref. [2].

169 4. Conclusions

170 Knowledge of the Rényi and Tsallis entropies is important in studying various phenomena in many
 171 branches of science. This general fact was confirmed above by showing that, for example, the Rényi
 172 position components of the QR at any coefficient α qualitatively repeat the behavior of the AB energy
 173 spectrum in zero uniform magnetic fields what can be used for predicting the magnitude of the associated
 174 persistent currents. Among other findings, let us mention the equation for the lowest boundary of the
 175 dimensionless Rényi/Tsallis coefficient at which the corresponding momentum components do exist,
 176 Eq. (37), which shows that there is its abrupt jump when the topology of the structure changes from the
 177 singly- to doubly-connected one. Note that for the orbitals with their position densities concentrated
 178 far away from the origin (what mathematically means that $a \gg 1$ and/or $|m| \gg 1$), the threshold
 179 from Eq. (37) approaches asymptotically that of the QD what physically is explained by the negligible
 180 influence of the inner confining potential on their properties. Uncertainty relations for both entropies are
 181 independent of the uniform field B and become tight not only for the 2D Gaussians of the lowest QD
 182 orbital, Eqs. (10) with $m = 0$, but also they turn into the identity at $\alpha = 1/2$ for the QR $n = m = 0$
 183 level, which is the only state that reaches this saturation. In this way, earlier conjecture [31] about the
 184 uniqueness of this orbital that should have the lowest energy is amended since the well-known property
 185 of the QR energy spectrum is crossings of the levels as the field B increases.

Flexibility of the model described by the potential from Eq. (1) leads to miscellaneous limiting geometries [2,6,7]; in particular, keeping constant the radius $r_{min} = 2^{1/2}a^{1/4}r_0$ at which the sole zero minimum of $U(r)$ is achieved and simultaneously unrestrictedly enlarging ω_0 , one arrives at the 1D ring of the same radius r_{min} pierced by the total magnetic flux $\phi_{tot} = \pi r_{min}^2 B + \phi_{AB}$ [64–67] when the position

waveform, Eq. (5a), energy spectrum, Eq. (11), and persistent current, Eq. (12), degenerate, respectively, to

$$\Psi_m(\varphi_r) = \frac{1}{(2\pi)^{1/2}} e^{im\varphi_r} \quad (56a)$$

$$E_m(\theta) = \frac{\hbar^2}{2m^*r_{min}^2} (m + \theta)^2 \quad (56b)$$

$$J_m = -\frac{e\hbar}{m^*r_{min}^2} (m + \theta), \quad (56c)$$

186 with $\theta = \phi_{tot}/\phi_0$. Observe that due to the frozen radial motion, the principal quantum index n has
 187 been dropped from Eqs. (56). Since $\Psi_m(\varphi_r)$ and $[2m^*E_m(\theta)]^{1/2}$ describe the eigenstates of the angular
 188 momentum of this AB rotator, the corresponding Rényi uncertainty relation is saturated by them and
 189 does not depend on α and β [29]. Let us also note that this model apparently can be used as a foundation
 190 of the quantum-informational analysis of the relevant more complicated structures, such as, for example,
 191 nanohelices [68–71].

Armed with the expression for the Rényi entropies, one can build up shape Rényi complexities [72]:

$$C_{\rho,\gamma}(\alpha) = e^{R_{\rho,\gamma}(\alpha)} O_{\rho,\gamma}, \quad (57)$$

192 where the formulas for the disequilibria $O_{\rho,\gamma}$ are given in Eqs. (15); for example, this was very recently
 193 done for a noncommutative anisotropic oscillator in a homogeneous magnetic field [73]. Regarding this
 194 dimensionless quantity, let us just to point out that for our geometry neither its position C_ρ nor wave
 195 vector C_γ component depends on the uniform intensity B .

196 Finally, let us remark that above the Rényi and Tsallis functionals were considered in the position and
 197 momentum spaces, which are two non-commuting observables. In the last year or so, Rényi [74,75] and
 198 Tsallis [75] entropies were proposed in energy and time domains; in particular, corresponding uncertainty
 199 relations were derived [74,75]. Application of these measures and associated inequalities to the analysis
 200 of the QDs and QRs may present an interesting development of quantum information and quantum
 201 cryptography protocols.

202 **Funding:** This research was funded by the Research Funding Department, Vice Chancellor for Research and
 203 Graduate Studies, University of Sharjah, SEED Project No. 1702143045-P.

204 **Conflicts of Interest:** The author declares no conflict of interest.

205 Abbreviations

206 The following abbreviations are used in this manuscript:

207	AB	Aharonov-Bohm
	n D	n -dimensional
208	QD	Quantum Dot
	QR	Quantum Ring

209 References

- 210 1. Fomin, V.M. *Physics of Quantum Rings*; Springer: Berlin, Germany, 2014.
- 211 2. Olendski, O. Quantum information measures of the Aharonov–Bohm ring in uniform magnetic fields. *Phys. Lett. A* **2019**, *383*, 1110–1122.

- 213 3. Aharonov, Y.; Bohm, D. Significance of electromagnetic potentials in the quantum theory. *Phys. Rev.* **1959**, *115*,
214 485–491.
- 215 4. Shannon, C.E. A mathematical theory of communication. *Bell Syst. Tech. J.* **1948**, *27*, 379–423.
- 216 5. Bogachek, E.N.; Landman, U. Edge states, Aharonov-Bohm oscillations, and thermodynamic and spectral
217 properties in a two-dimensional electron gas with an antidot. *Phys. Rev. B* **1995**, *52*, 14067.
- 218 6. Tan, W.-C.; Inkson, J.C. Landau quantization and the Aharonov-Bohm effect in a two-dimensional ring. *Phys.*
219 *Rev. B* **1996**, *53*, 6947–6950.
- 220 7. Tan, W.-C.; Inkson, J.C. Electron states in a two-dimensional ring - an exactly soluble model. *Semicond. Sci.*
221 *Technol.* **1996**, *11*, 1635–1641.
- 222 8. Tan, W.-C.; Inkson, J.C. Magnetization, persistent currents, and their relation in quantum rings and dots. *Phys.*
223 *Rev. B* **1999**, *60*, 5626–5635.
- 224 9. Fukuyama, H.; Sasaki, T.; Yokoyama, K.; Ishikawa, Y. Orbital magnetism in two-dimensional systems. *J. Low*
225 *Temp. Phys.* **2002**, *126*, 1067–1080.
- 226 10. Bulaev, D.V.; Geyler, V.A.; Margulis, V.A. Effect of surface curvature on magnetic moment and persistent
227 currents in two-dimensional quantum rings and dots. *Phys. Rev. B* **2004**, *69*, 195313.
- 228 11. Simonin, J.; Proetto, C.R.; Barticevic, Z.; Fuster, G. Single-particle electronic spectra of quantum rings: a
229 comparative study. *Phys. Rev. B* **2004**, *70*, 205305.
- 230 12. Margulis, V.A.; Mironov, V.A. Magnitnyi moment kol'ca Volcano. *Fiz. Tverd. Tela (S.-Peterburg)* **2008**, *50*, 148–153
231 [English translation: Magnetic Moment of the Volcano ring. *Phys. Solid State* **2008**, *50*, 152–158].
- 232 13. Olendski, O.; Barakat, T. Magnetic field control of the intraband optical absorption in two-dimensional quantum
233 rings. *J. Appl. Phys.* **2014**, *115*, 083710.
- 234 14. Xiao, M.; Reyes-Serrato, A. Analytic Aharonov-Bohm rings: currents readout from Zeeman spectrum. *Int. J.*
235 *Mod. Phys. B* **2016**, *30*, 1650106.
- 236 15. Negrete, O.A.; Peña, F.J.; Vargas, P. Magnetocaloric effect in an antidot: the effect of the Aharonov-Bohm flux
237 and antidot radius. *Entropy* **2018**, *20*, 888.
- 238 16. Abramowitz, M.; Stegun, I.A. *Handbook of Mathematical Functions*; Dover, New York, USA, 1964.
- 239 17. Gradshteyn, I.S.; Ryzhik, I.M. *Table of Integrals, Series, and Products*, 8th ed.; Academic Press, New York, USA,
240 2014.
- 241 18. Białyński-Birula, I.; Mycielski, J. Uncertainty relations for information entropy in wave mechanics. *Commun.*
242 *Math. Phys.* **1975**, *44*, 129–132.
- 243 19. Beckner, W. Inequalities in Fourier analysis. *Annals Math.* **1975**, *102*, 159–182.
- 244 20. Büttiker, M.; Imry, Y.; Landauer, R. Josephson behavior in small normal one-dimensional rings. *Phys. Lett. A*
245 **1983**, *96*, 365–367.
- 246 21. Rényi, A. On Measures of Entropy and Information. In *Contributions to the Theory of Statistics*, Proceedings of the
247 Fourth Berkeley Symposium on Mathematical Statistics and Probability, vol. 1, University of California, USA,
248 20 June–30 July 1960; Neyman, J., Ed.; University of California Press: Berkeley, USA, 1961; 547–561.
- 249 22. Rényi, A. *Probability Theory*; North-Holland: Amsterdam, The Netherlands, 1970.
- 250 23. Tsallis, C. Possible generalization of Boltzmann-Gibbs statistics. *J. Stat. Phys.* **1988**, *52*, 479–487.
- 251 24. Havrda, J.; Charvát, F. Quantification method of classification processes. Concept of structural α -entropy.
252 *Kybernetika* **1967**, *3*, 30–35.
- 253 25. Daróczy, Z. Generalized information functions. *Inform. Control* **1970**, *16*, 36–51.
- 254 26. Onicescu, O. Énergie informationnelle. *C. R. Acad. Sci. Ser. A* **1966**, *263*, 841–842.
- 255 27. Beckner, W. Inequalities in Fourier analysis on R^n . *P. Natl. Acad. Sci. USA* **1975**, *72*, 638–641.
- 256 28. Rajagopal, A.K. The Sobolev inequality and the Tsallis entropic uncertainty relation. *Phys. Lett. A* **1995**, *205*,
257 32–36.
- 258 29. Białyński-Birula, I. Formulation of the uncertainty relations in terms of the Rényi entropies. *Phys. Rev. A* **2006**,
259 *74*, 052101.
- 260 30. Zozor, S.; Vignat, C. On classes of non-Gaussian asymptotic minimizers in entropic uncertainty principles.
261 *Physica A* **2007**, *375*, 499–517.

- 262 31. Olendski, O. Rényi and Tsallis entropies: three analytic examples. *Eur. J. Phys.* **2019**, *40*, 025402.
- 263 32. Jizba, P.; Arimitsu, T. The world according to Rényi: thermodynamics of multifractal systems. *Ann. Phys. (N.Y.)*
264 **2004**, *312*, 17–59.
- 265 33. Jizba, P.; Dunningham, J.A.; Joo, J. Role of information theoretic uncertainty relations in quantum theory. *Ann.*
266 *Phys. (N.Y.)* **2015**, *355*, 87–115.
- 267 34. Tsallis, C. *Introduction to Nonextensive Statistical Mechanics*; Springer: New York, USA, 2009.
- 268 35. Tsallis, C. The nonadditive entropy S_q and its applications in physics and elsewhere: some remarks. *Entropy*
269 **2011**, *13*, 1765–1804.
- 270 36. Geilikman, M.B.; Golubeva, T.V.; Pisarenko, V.F. Multifractal patterns of seismicity. *Earth Planet. Sci. Lett.* **1990**,
271 *99*, 127–132.
- 272 37. Carranza, M.L.; Acosta, A.; Ricotta, C. Analyzing landscape diversity in time: the use of Rényi's generalized
273 entropy function. *Ecol. Indic.* **2007**, *7*, 505–510.
- 274 38. Rocchini, D.; Delucchi, L.; Bacaro, G.; Cavallini, P.; Feilhauer, H.; Foody, G.M.; He, K.S.; Nagendra, H.; Porta,
275 C.; Ricotta, C.; Schmidlein, S.; Spano, L.D.; Wegmann, M.; Neteler, M. Calculating landscape diversity with
276 information-theory based indices: a GRASS GIS solution. *Ecol. Inf.* **2013**, *17*, 82–93.
- 277 39. Drius, M.; Malavasi, M.; Acosta, A.T.R.; Ricotta, C.; Carranza, M.L. Boundary-based analysis for the assessment
278 of coastal dune landscape integrity over time. *Appl. Geogr.* **2013**, *45*, 41–48.
- 279 40. Rosso, O.A.; Martin, M.T.; Figliola, A.; Keller, K.; Plastino, A. EEG analysis using wavelet-based information
280 tools. *J. Neurosci. Meth.* **2006**, *153*, 163–182.
- 281 41. Tozzi, A.; Peters, J.F.; Çankaya, M.N. The informational entropy endowed in cortical oscillations. *Cogn.*
282 *Neurodyn.* **2018**, *12*, 501–507.
- 283 42. Costa, M.; Goldberger, A.L.; Peng, C.-K. Multiscale entropy analysis of biological signals. *Phys. Rev. E* **2005**, *71*,
284 021906.
- 285 43. Aptekarev, A.I.; Dehesa, J.S.; Sánchez-Moreno, P.; Tulyakov, D.N. Rényi entropy of the infinite well potential in
286 momentum space and Dirichlet-like trigonometric functionals. *J. Math. Chem.* **2012**, *50*, 1079–1090.
- 287 44. Toranzo, I.V.; Dehesa, J.S. Rényi, Shannon and Tsallis entropies of Rydberg hydrogenic systems. *Europhys. Lett.*
288 **2016**, *113*, 48003.
- 289 45. Dehesa, J.S.; Toranzo, I.V.; Puertas-Centeno, D. Entropic measures of Rydberg-like harmonic states. *Int. J.*
290 *Quantum Chem.* **2016**, *117*, 48–56.
- 291 46. Aptekarev, A.I.; Tulyakov, D.N.; Toranzo, I.V.; Dehesa, J.S. Rényi entropies of the highly-excited states of
292 multidimensional harmonic oscillators by use of strong Laguerre asymptotics. *Eur. Phys. J. B* **2016**, *89*, 85.
- 293 47. Nasser, I.; Zeama, M.; Abdel-Hady, A. The Rényi entropy, a comparative study for He-like atoms using the
294 exponential-cosine screened Coulomb potential. *Results Phys.* **2017**, *7*, 3892–3900.
- 295 48. Mukherjee, N.; Roy, A.K. Information-entropic measures in free and confined hydrogen atom. *Int. J. Quantum*
296 *Chem.* **2018**, *118*, e25596.
- 297 49. Mukherjee, N.; Roy, A.K. Information-entropic measures in confined isotropic harmonic oscillator. *Adv. Theory*
298 *Simul.* **2018**, *1*, 1800090.
- 299 50. Ou, J.-H.; Ho, Y.K. Benchmark calculations of Rényi, Tsallis entropies, and Onicescu information energy for
300 ground state helium using correlated Hylleraas wave functions. *Int. J. Quantum Chem.* **2019**, *119*, e25928.
- 301 51. Zeama, M.; Nasser, I. Tsallis entropy calculation for non-Coulombic helium. *Physica A* **2019**, *528*, 121468.
- 302 52. Ou, J.-H.; Ho, Y.K. Shannon, Rényi, Tsallis entropies and Onicescu information energy for low-lying singly
303 excited states of helium. *Atoms* **2019**, *7*, 70.
- 304 53. Klebanov, I.R.; Pufu, S.S.; Sachdev, S.; Safdi, B.R. Rényi entropies for free field theories. *J. High Energy Phys.*
305 **2012**, *2012*, 74.
- 306 54. Chen, B.; Zhang, J. On short interval expansion of Rényi entropy. *J. High Energy Phys.* **2013**, *2013*, 164.
- 307 55. Dong, X. The gravity dual of Rényi entropy. *Nature Commun.* **2016**, *7*, 12472.
- 308 56. Islam, R.; Ma, R.; Preiss, P.M.; Tai, M.E.; Lukin, A.; Rispoli, M.; Greiner, M. Measuring entanglement entropy in
309 a quantum many-body system. *Nature (London)* **2015**, *528*, 77–83.

- 310 57. Kaufman, A.M.; Tai, M.E.; Lukin, A.; Rispoli, M.; Schittko, R.; Preiss, P.M.; Greiner, M. Quantum thermalization
311 through entanglement in an isolated many-body system. *Science*, **2016**, *353*, 794–800.
- 312 58. Brydges, T.; Elben, A.; Jurcevic, P.; Vermersch, B.; Maier, C.; Lanyon, B.P.; Zoller, P.; Blatt, R.; Roos, C.F. Probing
313 Rényi entanglement entropy via randomized measurements. *Science* **2019**, *364*, 260–263.
- 314 59. Fikhtengol'ts, G.M. *The Fundamentals of Mathematical Analysis*, vol. 2, Pergamon: Oxford, UK, 1965.
- 315 60. Prudnikov, A.P.; Brychkov, Y.A.; Marichev, O.I. *Integrals and Series*, vol. 2, Gordon and Breach: New York, USA,
316 1992.
- 317 61. Wehner, S.; Winter, A. Entropic uncertainty relations - a survey. *New J. Phys.* **2010**, *12*, 025009.
- 318 62. Coles, P.J.; Berta, M.; Tomamichel, M.; Wehner, S. Entropic uncertainty relations and their applications. *Rev.*
319 *Mod. Phys.* **2017**, *89*, 015002.
- 320 63. De Palma, G.; Trevisan, D.; Giovannetti, V.; Ambrosio, L. Gaussian optimizers for entropic inequalities in
321 quantum information. *J. Math. Phys.* **2018**, *59*, 081101.
- 322 64. Aharonov, Y.; Bohm, D. Further considerations on electromagnetic potentials in the quantum theory. *Phys. Rev.*
323 **1961**, *123*, 1511–1524.
- 324 65. Merzbacher, E. Single valuedness of wave functions. *Am. J. Phys.* **1962**, *30*, 237–247.
- 325 66. Feinberg, E.L. Ob "osoboi" roli elektromagnitnykh potencialov v kvantovoi mechanike. *Usp. Fiz. Nauk* **1962**, *78*,
326 53–64 [English translation: On the "special role" of the electromagnetic potentials in quantum mechanics. *Phys.*
327 *- Usp.* **1962**, *5*, 753–760].
- 328 67. Peshkin, M. Aharonov-Bohm effect in bound states: theoretical and experimental status. *Phys. Rev. A* **1981**, *23*,
329 360–361.
- 330 68. Tinoco Jr., I.; Woody, R.W. Optical rotation of oriented helices. IV. A free electron on a helix, *J. Chem. Phys.* **1964**,
331 *40*, 160–165.
- 332 69. Kibis, O.V.; Malevannyy, S.V.; Huggett, L.; Parfitt, D.G.W.; Portnoi, M.E. Superlattice properties of helical
333 nanostructures in a transverse electric field. *Electromagnetics* **2005**, *25*, 425–435.
- 334 70. Vorobyova, J.S.; Vorob'ev, A.B.; Prinz, V.Y.; Toropov, A.I.; Maude, D.K. Magnetotransport in two- dimensional
335 electron gas in helical nanomembranes. *Nano Lett.* **2015**, *15*, 1673–1678.
- 336 71. Downing, C.A.; Robinson, M.G.; Portnoi, M.E. Nanohelices as superlattices: Bloch oscillations and electric
337 dipole transitions. *Phys. Rev. B* **2016**, *94*, 155306.
- 338 72. Antolín, J.; López-Rosa, S.; Angulo, J.C. Rényi complexities and information planes: atomic structure in
339 conjugated spaces. *Chem. Phys. Lett.* **2009**, *474*, 233–237.
- 340 73. Nath, D.; Chosh, P. A generalized statistical complexity based on Rényi entropy of a noncommutative
341 anisotropic oscillator in a homogeneous magnetic field. *Int. J. Mod. Phys. A* **2019**, *34*, 1950105.
- 342 74. Coles, P.J.; Katariya, V.; Lloyd, S.; Marvian, I.; Wilde, M. M. Entropic energy-time uncertainty relation. *Phys.*
343 *Rev. Lett.* **2019**, *122*, 100401.
- 344 75. Rastegin, A. E. On entropic uncertainty relations for measurements of energy and its "complement". *Ann. Phys.*
345 *(Berlin)* **2019**, *531*, 1800466.